ACS APPLIED BIO MATERIALS

www.acsabm.org Article

Tailored Biofunctionalized Biosensor for the Label-Free Sensing of Prostate-Specific Antigen

Sachin Mishra, Eun-Seong Kim, Parshant Kumar Sharma, Zhi-Ji Wang, Sung-Hyun Yang, Ajeet Kumar Kaushik, Cong Wang,* Yang Li,* and Nam-Young Kim*

Cite This: https://dx.doi.org/10.1021/acsabm.0c01002 Read Online

ACCESS | Metrics & More | Article Recommendations | Supporting Information

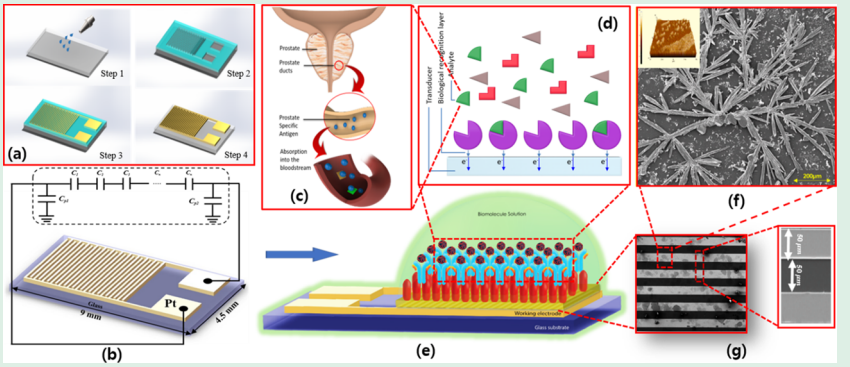

ABSTRACT: The increase in the demand and popularity of smart biosensors has brought a novel and innovative concept to develop a diverse range of semen mutual biomarker (i.e., prostate-specific antigen, PSA)-based biodevices for our daily life applications. Using a versatile strategy, here we have developed a next-generation miniaturized capacitive biomarker-based sensor, which facilitates a direct, rapid quantitation and ultrafast detection of prostate-specific antigen (PSA) selectively. To fabricate an affordable PSA biosensor, an interdigitated capacitor (IDC) was functionalized and to detect PSA at concentrations varying from 0.1 to 10 μL/mL, with a response time of 3 s. Moreover, the PSA biosensor showed a high level of selectivity due to the successful probing of the capacitive response-generated biomolecular interactions using external stimuli at the bioelectrode. The resulting IDC-based PSA biosensors are capable of excellent reproducibility and reusability, which are required for real-time biosensing of any targeted biomolecules where low-concentration detection is a key for point-of-care, on-site sensing applications. We anticipate that this research could open exciting opportunities for PSA detection at a low concentration level.

KEYWORDS: *prostate cancer, biosensor, prostate-specific antigen, interdigitated capacitor (IDC), point-of-care, reusability*

1. INTRODUCTION

Prostate cancer (PCa) is a common cancer malignancy among male populations and a major cause of cancer mortality globally.[1−4] The progress of PCa understanding, investigation of symptom progression, and designing new therapies of PCa treatment always rely on monitoring and recognition of semen-based targeted biomarkers, namely, prostate-specific antigen (PSA), associated with PCa.[5−9] PSA is considered to belong to the human glandular kallikrein 2 (or hK2) family that has a chymotrypsin-like serine protease enzymatic activity. PSA occurs in two different forms, i.e., free and protease inhibitor-bound, and it is possible to determine the ratios of the two respective forms using the clinical detection of PCa. The androgen-regulated PSA is induced by the prostatic tissue and released into the lumen. PSA is a major protein found in semen and its functions is to cleave semenogelins present in the seminal coagulum. Also, the level of PSA is eventually increased in the serum of prostate cancer (PCa) patients. For this reason, the proteolytic activity suffers when the serum protease inhibitors form irreversible complexes. PCa detection test are conducted when the PSA value is ≥4.0 ng/mL in the prostate gland.[10]

Although PSA is not considered as a PCa biomarker since the PSA content in the serum might also increase in other noncancerous diseases of the prostate,[11,12] the lack of other biomarkers turned the focus onto efficient PSA detection (Table S1) for early-stage detection of PCa and therapy efficacy.[13] Considering the significance, ultrasensitive detection

Received: August 10, 2020
Accepted: October 15, 2020

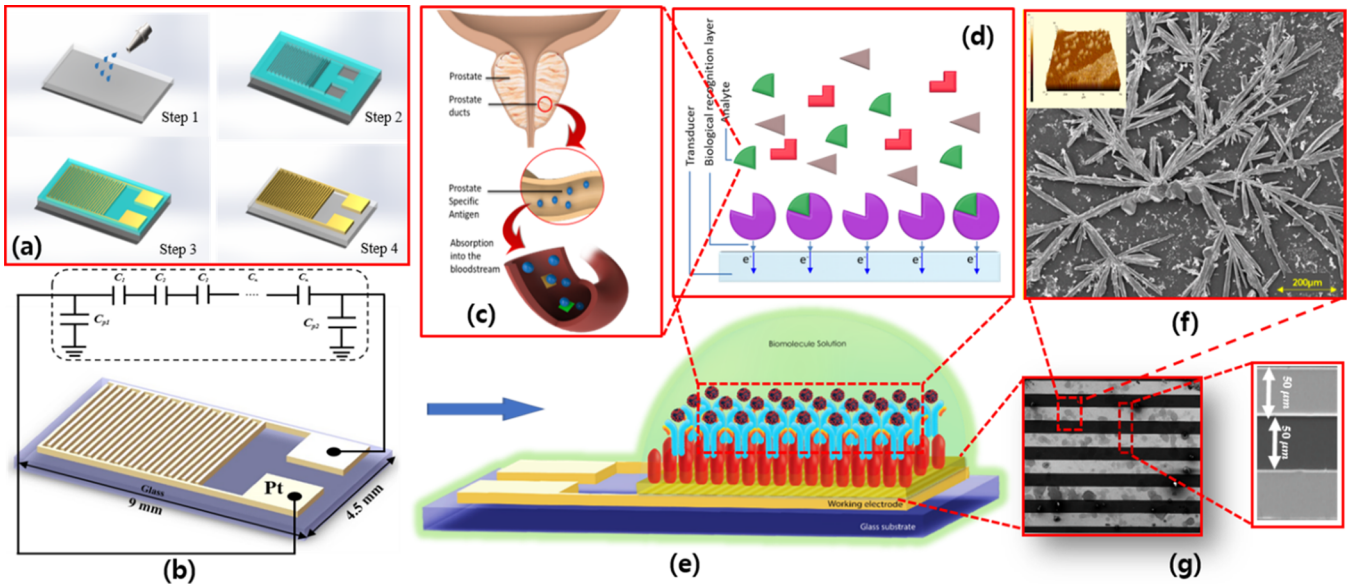

Figure 1. Schematic representation of the high-sensitivity and reusable prostate-specific-antigen-based capacitive biosensor: (a) design and simulation of the IDC biosensor chip having 24 fingers and interdigitated capacitor arrays of 100 μm width and 100 μm finger gap implemented using the ADS method and fabricated onto glass wafers. Step 1: the glass wafer substrate of 700 μm thickness is cleaned using an ultrasonic acetone bath at an acid wet station for the e-beam deposition process. Step 2: a metal layer was uniformly coated onto the glass wafer via the spin-coating method; then, acid cleaning of the surface was performed. Step 3: this deposition process was executed under a certain pressure. Step 4: finally, the photoresist was removed using a lift-off machine with acetone/IPA/DI water in 90 s. In the simulation, a frequency of 1 MHz for 3.75 pF was applied by Advance Design System (ADS Keysight) software. (b) Fabricated interdigitated capacitor (IDC) biochip layout. (c) Illustrative overview of the PSA biomolecules that are released by the prostate gland.[47] (d) PSA acts as an analyte in the biosensor component to accelerate the mechanism for the detection of respective biomarkers. (e) Setup of the biochip. (f) Morphological behavior of the biochip in the presence of anti-PSA binding with the biological system. (g) Scanning image signifies the presence of PSA on the surface and defines the measurement between two metal fingers, i.e., 100 μm.

of PSA at pg/mL volume led to the early-stage detection of PCa, smart diagnosis, and nonrecurrence of the disease.[14,15]

Classical analytical approaches (Table S2) for PSA detection include radioimmunoassay,[16] fluorescence method,[17] enzyme-linked immunosorbent assay (ELISA),[18] surface plasmon resonance (SPR),[19] electrochemiluminescence (ECL) immunoassay,[20] surface-enhanced Raman scattering (SERS),[21] and electrochemical methods.[22] The above methods have made significant accomplishments but are expensive, need an expert for operation, good laboratory setup, and several bioreagents, which limit their application for timely PCa diagnosis[23,24] (Tables S3 and S4). Among several types of biosensors, electrochemical biosensing approaches have emerged as a potential solution because of the affordability, easy fabrication processes, and tunable signal amplification using appropriate transduction, micro/nanoelectronics, and surface-functionalized nanosystems.[25] These salient features allowed scientists to develop several types of PSA biosensors, for example, aptamer-based optical and electrical PSA biosensors[26,27] or electrochemical biosensors.[10,28,29] Aptamer or nucleic acid emerged as the desired bioactive compound to fabricate a sensitive nanoenabled genosensor because it can immobilize on the nanosurface and selectively bind with the targeted biological elements and complex species such as living cells.[30] Due to the above features, aptamer-based biosensors exhibited high binding affinity, specificity, and a wide range of detection concentrations.[31] Besides, poor stability and expensive diagnostics still remain as challenges to overcome. These features in an analytical diagnostic tool are a must for managing PCa at the point of care (POC) and according to patient profiles, i.e., personalized health management.[32−35]

Considering the above discussion as motivation, this research, for the first time, demonstrates the fabrication of a tailored biofunctionalized interdigitated capacitor (IDC) biosensor for label-free PSA detection. The miniaturized IDC-PSA biosensor exhibited PSA detection at low levels within 3 s of response time. Such desired sensitivity and selectivity sensing features are suitable for transforming our fabricated IDC-PSA biosensor to achieve PSA detection at the POC. The IDC-PSA biosensor is affordable ($ < 5.00) and easy to operate and has a very superior advantage of reusability, which makes the diagnosis more affordable. The results of our research confirmed the superior and practical advantages of the fabricated IDC-PSA biosensor when compared with the available sensing system-based screen-printed electrode (SPE) technology.

A sandwich-architecture-based label-free PSA sensing system was also configured to assess the performance of the IDC-PSA biosensor in human semen in a real-time manner with the reduced form factors (mainly the response time of a few seconds). According to the current research outcomes, the PSA-based biosensor acts as a smart IDC chip with expanded biointerfaces, opens a new way to detect targeted biological samples, even for point-of-care applications.

2. EXPERIMENTAL SECTION

2.1. Materials. All stock solutions were prepared using deionized water obtained using a Milli-Q device supplied with a water dispenser system from Simplicity, Millipore (USA). Anti-prostate-specific antigen antibody produced in rabbit (product number SAB4501531) and prostate-specific antigen procured from human semen (product number P3338-25UG) were obtained from Sigma-Aldrich. Sulfuric acid (H_2SO_4), hydrogen peroxide (H_2O_2), 3-

https://dx.doi.org/10.1021/acsabm.0c01002
ACS Appl. Bio Mater. XXXX, XXX, XXX−XXX

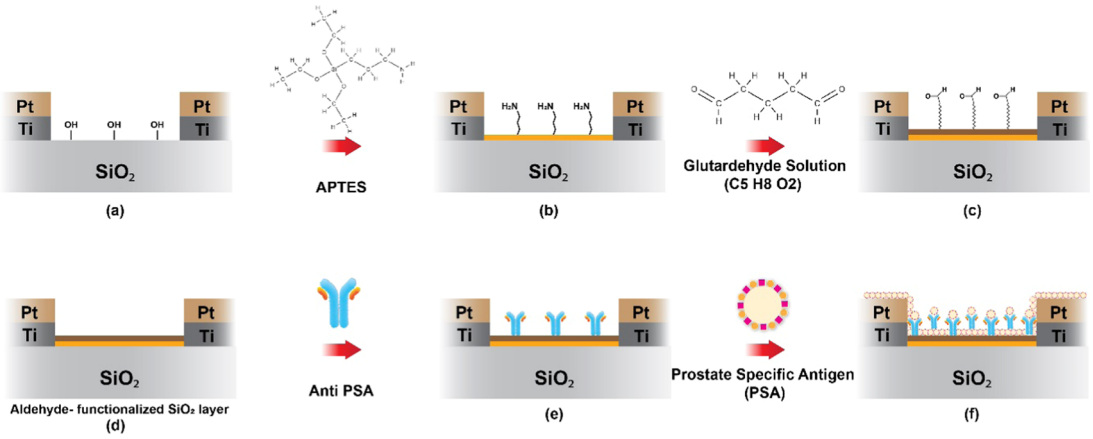

Figure 2. (a–f) Subsequent process of the fabrication of IDC biosensors. Surface modification, Aβ antibody immobilization, and PSA binding on the surface.

aminopropyltriethoxysilane (99%, APTES), and glutaraldehyde solution (Grade I, 70% in H_2O) were purchased from Sigma-Aldrich. Phosphate-buffered saline (PBS) buffer solution (0.1×, pH 7.4) and ethyl alcohol were also used. An impedance analyzer or an LCR meter (an instrument used to measure the inductance (L), capacitance (C), and resistance (R) of an electronic component) was utilized to characterize the sandwich-type bioelectrodes and estimate the PSA concentration levels. Capacitive measurements were carried out in a frequency range within 1–100 kHz.

2.2. Simulation and Fabrication of the IDC Chip. To design an IDC sensor, which has 24 fingers, interdigitated capacitor arrays with 100 μm width and 100 μm finger gap were implemented using the simulation software (Advance Design System (ADS)) (Figure S1) and fabricated onto Eagle XG glass wafers using image reversal photolithography for pattern transfer. The Eagle XG glass substrate of 700 μm thickness is cleaned with isopropyl alcohol (IPA) and using an ultrasonic acetone bath at an acid wet station with a mixture of HCL and H_2O in the ratio of 1:10 for 60 s (Figure 1a; Step 1) for the Ti/Pt e-beam deposition process. This cleaning process is very important for effective photoresist coating for Ti/Pt metal deposition. Without the proper cleaning process, the deposited Ti/Pt metal is easily lifted off together with the photoresist coating. In the next step, a spin-coater was used to spin a negative photoresist onto a glass wafer substrate with a thickness of 3 μm; then, the edge bead removal process was applied to make sure the coated resist's thickness was uniform to deposit the metal layer. Then, the acid cleaning of the surface was performed (Figure 1a; Step 2). In the e-beam deposition process, first Ti is attached onto the glass substrate and then Pt is deposited on Ti because Pt cannot be attached onto the glass surface directly. In the second e-beam process, Ti/Pt is deposited with the thicknesses of Ti and Pt being 0.15 and 0.15 μm, respectively. This deposition process was achieved under a pressure of 5.0×10^{-6} mTorr, and the electron energy was fixed at 10 kV. Moreover, a minimum deposition rate of 0.5 Å/s was set to obtain an accurate layer thickness (Figure 1a; Step 3). Finally, the photoresist was removed using a lift-off machine with acetone/IPA/DI water in 90 s (Figure 1a; Step 4). In the simulation, we set the frequency to 1 MHz for 3.75 pF and the measurement result was 3.8 pF. Advance Design System (ADS Keysight©) software is used for a 4.5×9 mm^2 size interdigitated capacitor (IDC) biochip layout (Figure 1b). The fabricated IDC is shown in the inset of Figure 1b with W_e = 100 μm, W_c = 100 μm, G_e = 100 μm, G_c = 100 μm, and L = 3.8 mm. Finally, the IDC is designed and fabricated as a capacitive biosensor to detect biosamples with high sensitivity (Figure S2). The IDC is measured by the LCR meter (*Handheld*, 1 kHz, 2 kHz, 200 pF, 0.2 Gohm, U1730C Series), which interfaces with a PC for data acquisition (Figure S3). The measurement was made with 0 V DC bias voltage and 1 kHz frequency across the IDC biosensor.

2.3. Characterization and Measurement. The surface characterization of the biocomposite was done in tapping mode using an atomic force microscope (AFM, Model XE-100, Park Systems, Korea). The appearance of thickness and surface modifications was recognized under a high-resolution low-vacuum scanning electron microscopy (SEM, FEI (Nova Nano SEM 200)). The prepared sample grids were viewed by a Fourier transform infrared (FT-IR) iS 10 (Thermo Fisher Scientific) at KIST (Korea Institute of Science and Technology). Capacitive measurements of the fabricated bioelectrode were made using an LCR meter (Gohm, U1730C Series) under dry conditions. The measurement was made with a 0 V DC bias voltage and 1 kHz frequency across the IDC biosensor.

2.4. Sample Preparation of PSA Bioelectrodes. The IDC biosensor that creates a progressive era of ultrasensing reusable devices that allow expanded sensitivity, cost-effectiveness, short analysis times, and miniaturized domain-based detection is gaining significant interest as a label-free technique for the sensitive measurement of target analytes. The substrate was activated in the first step by placing the IDC surface into a Piranha solution for the piranha etching process consisting of treatment with a mixture of H_2O_2 and H_2SO_4 in a 1:1 ratio at 80 °C for 15–20 min to clean organic contaminants for optimal formation of hydroxyl groups at the surface (Figures 2a and S4). After cleaning with the Piranha solution, the surface was washed with Milli-Q water and ethanol. Next, 3-aminopropyltriethoxysilane solution (2 wt % APTES [3-amino-propyltriethoxysilane]); (Sigma-Aldrich) was drop-cast for 3 h for the formation of an amine functional group on the surface (Figure 2b); subsequently, 25% glutaraldehyde solution ($C_5H_8O_2$) was applied at room temperature (RT) for 3 h to generate an antibody through cross-linking (Figure 2c).[48,49] After the formation of the aldehyde group on the IDC surface (Figure 2d), the anti-prostate-specific antigen antibody produced in rabbit (10 μg/mL in PBS, pH 7.4) was fabricated overnight at room temperature (25 °C), as shown in Figure 2e. The formation of the chemical layer and the immobilization of the anti-PSA responded to capacitance changes caused by the binding of target analytes that are immobilized on the biochip. Figure 2f shows that the fabrication of the anti-PSA, further immobilization of PSA at different concentrations was performed at room temperature onto the biosurface to check the capacitance value using the LCR meter.

The IDC-based PSA biosensor shows a positive capacitive response after the addition of APTES and incubation with glutaraldehyde solution, and the value of capacitance increase due to the presence of APTES and glutaraldehyde solution that binds to the surface is treated as the reference value. Eventually, the capacitance variables are changed after the addition of the target protein (PSA) at different concentrations (in the range from 0.1 to 10 μL/mL) to the IDC biosensor, and the changes are calculated by the LCR meter (Gohm, U1730C Series) (Figure S5).

https://dx.doi.org/10.1021/acsabm.0c01002
ACS Appl. Bio Mater. XXXX, XXX, XXX–XXX

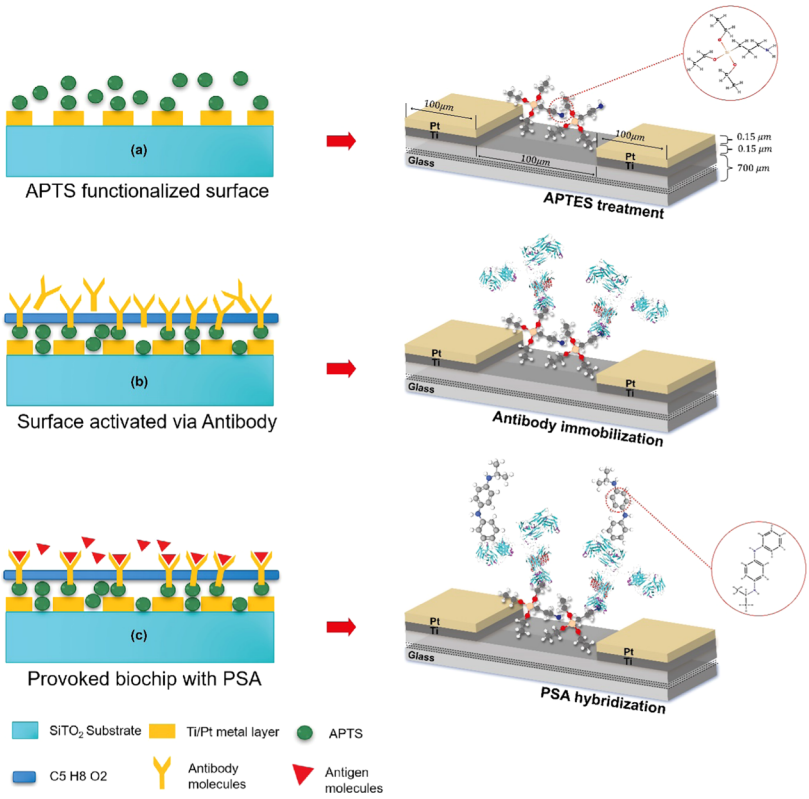

Figure 3. (a–c) Proposed schematics for the fabrication of the antibody–antigen interaction.

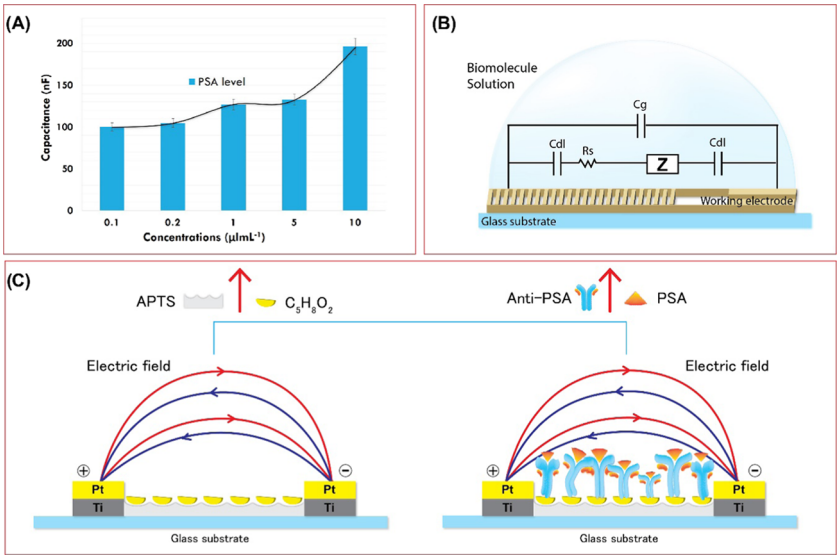

Figure 4. (A) Capacitance vs PSA concentration curve. (B) ADS simulation for the current density; an equivalent circuit of the capacitive coupling effect. (C) Ti/Pt-based IDC equivalent circuit bound by PSA biomolecules disrupting the electric field between the metal electrodes (metal fingers), causing a change illustrated in the capacitance vs concentration curve.[50−52]

The capacitance was calculated at each step, and the changes of the IDC biosensor were recorded using (a) Bare-APTES IDC sensing chip, (b) antibody immobilization, and (c) PSA fabrication (Figure 3). The biosurface was activated due to the rapid and nondestructive control of the biological systems and provided balanced and nondrifting signals in the presence of the complete biosensor insulation system. For the determination of the reusability of the capacitive biosensors, PSA was detected repeatedly at the same capacitance value under the mentioned conditions, which signifies the biosensor chip regained the original capacitive characteristics after rinsing with PBS solution and then drying. Reproducibility of the assays was evaluated by monitoring the change in the capacitance at different concentrations in the range of 0.1−10 μL/mL in a 3 s response time, which is quite a fast detection time for first-generation IDC biosensors compared with the values from the published literature.

The novel biosensor enables one to detect the capacitive sensitivity from pF to nF levels having standard PSA concentration ranges within a 3 s response time, as shown in Table S5. In the current paper, sandwich-based layer-by-layer arrangements in the label-free technique were used, and such a configuration allows real-time detection with a reduced time of analysis.

https://dx.doi.org/10.1021/acsabm.0c01002
ACS Appl. Bio Mater. XXXX, XXX, XXX−XXX

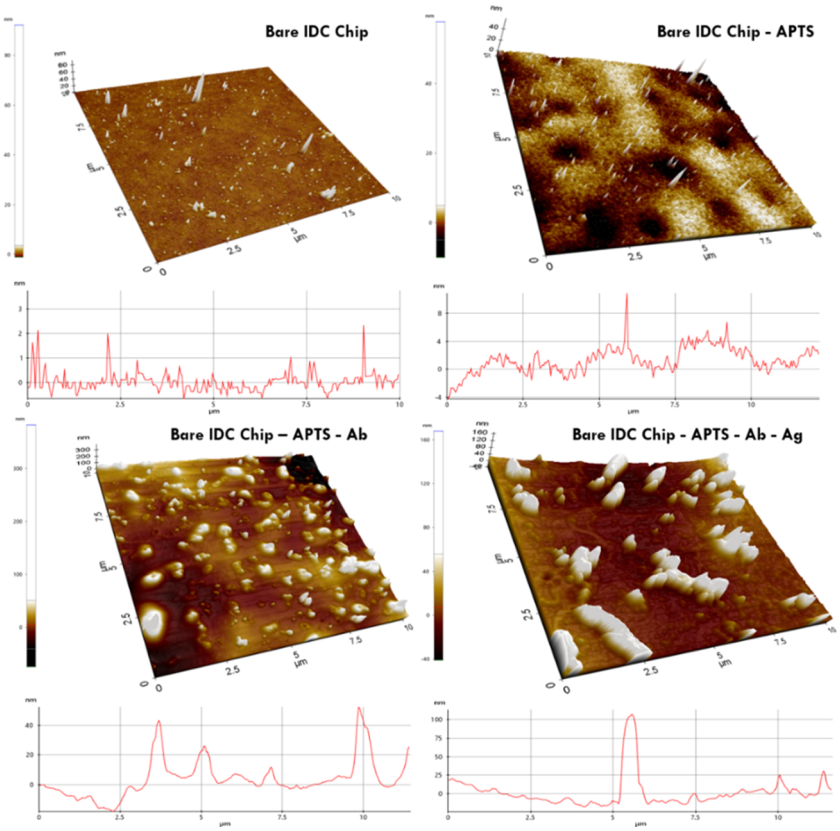

Figure 5. AFM images of the IDC glass chip along with functionalization with APTES, APTES-Ab, and APTES-Ab-Ag capacitive biochips.

The IDC biosensor is designed to detect properties of specific antigens and antibodies of PSA biomaterials. The main concept of the IDC biosensor for measuring the bioproperties is based on variations of three properties such as the charge distribution, dielectric constant, and conductivity. When an analyte is placed on an IDC substrate, the dielectric reacts, and charge distribution and conductivity in the presence of the antibody and antigen are also changed. Therefore, the sensing response of the IDC biosensor can be obtained by observing the capacitive reactance through the IDC voltage. The immobilized PSA antibody on the IDC surface was functionalized by a 2 wt % 3-aminopropyltriethoxysilane (APTES) solution. The substrate was characterized by Atomic force microscopy (AFM), Scanning electron microscopy (SEM), Fourier transform infrared (FT-IR) spectroscopy, and ultrafast capacitance measurements with different standard PSA concentrations of 0.1, 0.2,1.0, 5.0, and 10 μL/mL. The antibody–antigen binding shows capacitive alteration due to the presence of several PSA concentrations of the captured antigen with anti-PSA antibody onto the glass substrate that helps in the quantification.

Capacitance-based detection techniques have been shown to have a short response time with higher sensitivity compared to other detection methods. However, we enhanced the sensitivity as well as the selectivity of the capacitive biosensor with biological elements onto the glass substrate in between the defined Ti/Pt electrodes. So, this kind of a unique design yields more precise results. The biomechanism by which the PSA molecules affect the capacitance of the sensing system can be represented using the equivalent circuit representation model shown in Figure 4. This circuit is a combination of the Ti/Pt metal layer capacitance of the digitated electrodes (Cdl), the physical capacitance of the electrode (Cg), the resistance of the surrounding biomolecule solution (Rs), and the impedance introduced by the bound nanoparticles (Z). PSA is an extremely useful biomarker for the detection of prostate cancer (PCa) that can bind to a specific biological substance with extremely high specificity. It is typically structured to bind to the substrate and deliver high sensitivity, causing a change that is illustrated via the capacitance vs concentration curve in Figure 4.

3. RESULTS AND DISCUSSION

3.1. Surface Characterization of the Capacitive Biosensor Chip. We have characterized the surface modification of the IDC chip by capacitance measurements, AFM, SEM, and FT-IR. Electrode material and biologically enhanced substance modifications were all investigated. The capacitance results showed that the surface modification using APTES generally formed a void over the surface and resulted in a fluctuation in the capacitance. The adsorption of anti-PSA onto the existing APTES binding sites shows a gradual increase with a change in the capacitance value.[53] The implemented characterizations show that changes can be detected in different concentrations of PSA. We found that the Ti/Pt IDCs showed better performance. They showed a unique tendency under layer-by-layer surface modifications in comparison with other fabrication and simulation methods. However, Ti/Pt is user friendly and provides cheaper microfabrication of metal electrode fingers onto the glass substrate. It is also essential to admit that the electrode materials can also be modified based on the biological substances being detected for better flexibility and other positive aspects. Changes in substrate modification also change the capacitance variables, which allows us to determine the diversity in PSA concentrations more clearly.

3.2. Atomic Force Microscopy (AFM) Study. To characterize the surface of the bare IDC glass chip, Bare-APTES, Bare-APTES-Ab, and Bare-APTES-Ab-Ag capacitive biochips (Figure 5), Atomic force microscopy (AFM) was employed in tapping mode (AFM, model XE-100, Park Systems, Korea). Oscillation frequency (320.30 Hz) and vibration amplitude (1 V) were used as experimental

https://dx.doi.org/10.1021/acsabm.0c01002
ACS Appl. Bio Mater. XXXX, XXX, XXX–XXX

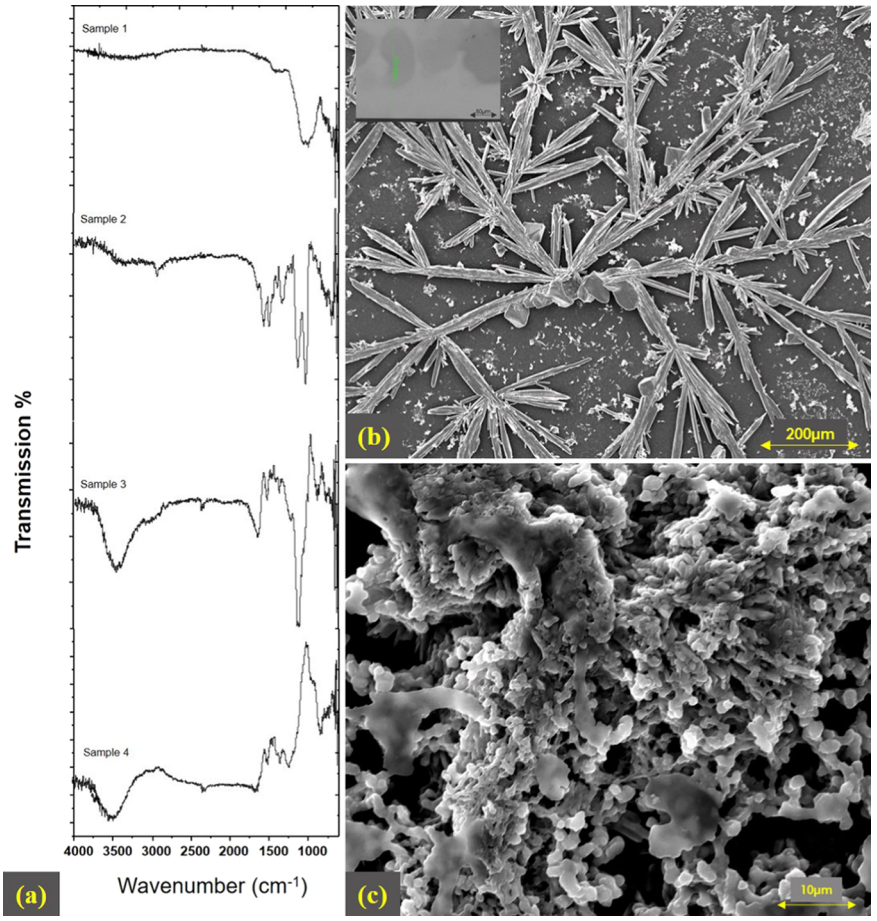

Figure 6. (a) FT-IR characterizations showing four different samples: bare chip, APTES-functionalized surface, antibody immobilization, and IDC-based PSA biochip. SEM characterizations. (b) Surface modification of the IDC chip by anti-PSA (inset: bare IDC chip) and (c) with PSA on the IDC glass substrate.

parameters (Figure S6). Imaging studies were performed at 2 mm/s scanning rate and 256 × 256 pixel resolution.

3.3. Fourier Transform Infrared Spectroscopy (FT-IR) and Scanning Electron Microscopy (SEM) Study. We confirmed the presence of the C−H aromatic ring with a weak intensity peak as well as C−H alkene, which is bent out of plane in the case of bare chip. Intermolecular sharp H bonds have been detected in the analysis. The results of FT-IR are shown in Figure 6a. In the spectrum, aliphatic C−H stretching bands at 849.82 cm^{-1} were observed (Figure S7). The figure shows four different steps for the bare biochip (Sample 1). In addition, the R−NO_2 nitro group and C−O (carboxyl ether) of the ethoxy group due to APTES immobilized on the biochip (Sample 2) are being observed; the figure also shows the biofunctionalized chip; O−H sharp peaks at 3612.48 and 1646 cm^{-1} indicate the presence of the nitro group due to the antibody on the surface (Sample 3); the figure also reveals the presence of PSA on the surface, and the R−NO_2 nitro group and C−O (carboxyl ether) and C−H aromatic peaks at 849−611 cm^{-1} (Sample 4) are also recognized. The spectra showed the specific bands corresponding to the O−H-bond- and C−H bond-modified IDC chips and the bands in the PSA-imprinted IDC biochip. Changes in the surface morphology of the IDC-based chip and the polymeric surface of the Ti\Pt-imprinted IDC biochip can be clearly seen in the SEM images of Figure 6b,c. The surface morphologies of the bare IDC glass chip (inset), anti-PSA, and PSA-based IDC glass substrate were observed by an ultrahigh-resolution low-vacuum scanning electron microscope (SEM, FEI (Nova Nano SEM 200)). The biochips were washed with ethanol and water for 10 min successively. Before SEM observation, the electrodes were sputter-coated with Au/Pd (Figure S8).

4. PSA DETECTION IN HUMAN SEMEN

To investigate the applicability and reliability of the PSA capacitive biosensors in clinical applications, recovery experiments were performed by the detection of PSA extracted from human semen. The results are shown in Table 1. The semen sample contains 26 kDa single-chain glycoprotein containing 237 amino acids, encoded by the kallikrein gene mapped to human chromosome 19. PSA detection at the μL/mL level (0.1−10.0) represents a successful result. A linear calibration curve obtained between the logarithm of the PSA concentration and the magnitude of capacitance response revealed a good linear range from 0.1 to 10 μL/mL and an excellent response at the low concentration of 0.1 μL/mL to the upper limit of 10 μL/mL with a correlation coefficient of 0.89 (Figure 7). Therefore, this detection limit indicates high detection sensitivity (0.1−10 μL/mL) in a short response time (3 s).

5. SELECTIVITY

To apply the developed functional biological composite anti-PSA-APTES-Pt/Ti-glass platform to determine PSA, its selectivity was tested against various potentially interfering

https://dx.doi.org/10.1021/acsabm.0c01002
ACS Appl. Bio Mater. XXXX, XXX, XXX−XXX

Table 1. Device Methods and Technical Specifications for PSA Biomarker Detection

sl.no	biomolecule(s) detected	types of devices	methods of detection	results readout	limits of detection	total detection time (min or s)	sample type	quantitative	ref(s)
1	glucose, nitrites, and protein	microfluidic paper-based analytical devices	chemical reactions with biomolecules and paper actuator	colorimetric	not available	12 min	artificial saliva	no	36
2	phenylalanine	microfluidic paper-based analytical devices	phe reaction forming NH_3 and pH change	colorimetric intensity	20 μM	20 min	urine	yes	37
3	glucose, pH, and protein	microfluidic paper-based analytical devices	enzymes and chromogenic agents	colorimetric	2 Mm, 0.6 mg/mL	5 min	artificial urine	yes	38
4	CRP	PDMS	capture antibodies	spectrometry shift	3.2 ng/mL	60 min	blood	yes	39
5	IL-2	PDMS	capture antibodies	fluorescence	50 pg/mL	30 min	blood	yes	40
6	myoglobin, cTn I, CK-MB	Cu microelectrode array on a glass chip	carbon nanotubes and antibodies	conductance	6 fg/mL, 50 fg/mL, 20 fg/mL	<1 min	spiked PBS	yes	41
7	insulin, glucagon, and somatostatin	Au layer on a glass chip	antibodies	surface plasmon resonance	1 nM, 4 nM, 246 nM	~20 min	spiked solution	yes	42
8	galectin-1	Au-plated glass chip	alumina nanoparticles, antibodies	impedance	7.8 μg/mL	30 min	T24 cell lysates	yes	43
9	IFN-γ	Au IDE-based chip	RNA aptamer on a gold electrode array	impedance	11.56 pM	<35 min	spiked solutions	yes	44
10	PSA	PDMS	polystyrene beads with antibodies	droplet counting	3.67 pM	45 min	spiked HEPES	yes	45
11	PSA	micropore filter paper on glass Chip	carbon nanotubes and antibodies	resistance	1.18 ng/mL	120 min	PSA solution	yes	46
this study	PSA	IDC on glass chip (yielding more than three times the capacity)	APTES and antibody	capacitance	0.1−10 μL/mL	03 s	human semen	yes	

https://dx.doi.org/10.1021/acsabm.0c01002
ACS Appl. Bio Mater. XXXX, XXX, XXX−XXX

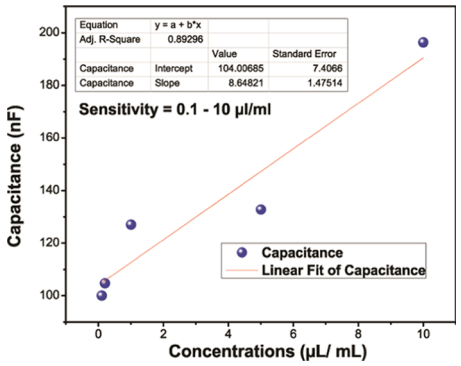

Figure 7. Linear calibration curve obtained between the logarithm of PSA concentration and the capacitance response. The graph shows a good linear range (R^2 = 0.89).

compounds coexisting in the biological samples such as glutaraldehyde solution ($C_5H_8O_2$). The tests were performed by measuring 0.1 and 10.0 μl/mL PSA standard solutions in the absence and presence of protein biomolecules. A change in the capacitance was proportional to the amount of PSA bound, as such allowing a highly specific and sensitive detection. The selectivity of the proposed biosensor chip was tested against different concentrations of PSA and the results confirmed the high selectivity of the developed biosensor toward PSA detection. Furthermore, the shelf-life (stability) of the sensor chip conjugated with glutaraldehyde solution ($C_5H_8O_2$) before and after testing with an anti-PSA, antibody aqueous solution was evaluated over the period of 15 days (Figure 8).

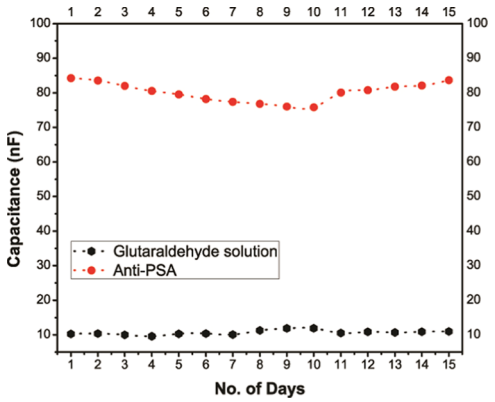

Figure 8. Shelf-life of the actual capacitive biosensor chip with glutaraldehyde solution ($C_5H_8O_2$) and anti-PSA antibody over a period of 15 days.

6. REUSABILITY OF THE PSA-IMPRINTED IDC BIOSENSOR

To demonstrate the reusability of the proposed PSA-imprinted IDC biosensor chip, its capacitance in different concentrations of standard PSA solutions was also evaluated. The results indicate that the biosensor chip regained the original resonance characteristics after washing in the Piranha solution at 80 °C and then drying. The IDC biosensor chip has a reusability of more than 3 times, which reduces its cost in the long term. The same IDC biosensor chip was used again, and each of the analyses was repeated up to three times. These results indicated that the stability of the PSA biosensor was satisfactory and there was no change in the capacitance with good reproducibility without a significant loss in the activity. The outcomes of this research suggest that the IDC-PSA capacitance sensor exhibits superior sensing performance, including detection in the physiological range, high sensitivity, good selectivity, fast response time, and excellent reusability, as summarized in Table 1 in comparison with reported PSA sensors.

7. CONCLUSIONS

In this research, a label-free capacitive biosensor was fabricated using a biofunctionalized IDC electrode (Ti/Pt imprinted) for selective and sensitive detection of PSA within 3 s. The IDC-PSA sensor was also configured to perform PSA detection in a real-time manner, which is required to manage at the POC according to the requirements of patient symptom progression. Such a PSA diagnosis requires a very low volume of sample and the sensor exhibited reproducibility and stability up to many weeks. Moreover, the novelty feature of reusability makes IDC-PSA biosensor acceptable to detect not only PSA but also other useful biomarkers, as well as perform early-stage diagnosis in a personalized manner. The tunable feature of the up-scaling capability using ordinary resources motivates us to transform the miniaturized IDC-PSA sensor for performing PCa diagnosis at the POC. We believe that the IDC-PSA biosensor can be part of a targeted disease management program where rapid, sensitive, and selective detection of biomarkers is urgently required in a highly sensitive and selective manner.

■ ASSOCIATED CONTENT

Supporting Information

The Supporting Information is available free of charge at https://pubs.acs.org/doi/10.1021/acsabm.0c01002.

ADS software design simulation of the proposed chip; the IDC process of layer fabrication; the complex permittivity in the IDC chip; the measurement preparation and schematic of the step illustration of the biochip through the layer deposition method; the capacitance value measurement at every fabrication step at room temperature; and surface modification characterization by atomic force microscopy (AFM), SEM, and FT-IR (PDF)

■ AUTHOR INFORMATION

Corresponding Authors

Cong Wang − *Department of Electronic Engineering, Kwangwoon University, Seoul 01897, South Korea; School of Electronics and Information Engineering, Harbin Institute of Technology, Harbin 150001, China*; Email: kevinwang@hit.edu.cn

Yang Li − *School of Electronics and Information Engineering, Harbin Institute of Technology, Harbin 150001, China; School of Information Science and Engineering, University of Jinan, Jinan 250022, China*; Email: sunny_lee2011@hotmail.com

Nam-Young Kim − *NDAC Centre and Department of Electronic Engineering, Kwangwoon University, Seoul 01897, South Korea; School of Electronics and Information Engineering, Harbin Institute of Technology, Harbin 150001, China*; Email: nykim@kw.ac.kr

https://dx.doi.org/10.1021/acsabm.0c01002
ACS Appl. Bio Mater. XXXX, XXX, XXX−XXX

Authors

Sachin Mishra − *NDAC Centre and Department of Electronic Engineering, Kwangwoon University, Seoul 01897, South Korea;* orcid.org/0000-0002-5132-9872

Eun-Seong Kim − *Department of Electronic Engineering, Kwangwoon University, Seoul 01897, South Korea*

Parshant Kumar Sharma − *Department of Electronic Engineering, Kwangwoon University, Seoul 01897, South Korea*

Zhi-Ji Wang − *Department of Electronic Engineering, Kwangwoon University, Seoul 01897, South Korea*

Sung-Hyun Yang − *Department of Electronic Engineering, Kwangwoon University, Seoul 01897, South Korea*

Ajeet Kumar Kaushik − *NanoBioTech Laboratory, Department of Natural Sciences, Division of Sciences, Arts, & Mathematics, Florida Polytechnic University, Lakeland, Florida 33805, United States;* orcid.org/0000-0003-4206-1541

Complete contact information is available at: https://pubs.acs.org/10.1021/acsabm.0c01002

Author Contributions

S.M. and E.-S.K. contributed equally to this work. The manuscript was written through contributions of all authors. All authors have given approval to the final version of the manuscript.

Funding

This research was partially funded by the Basic Science Research Program through the National Research Foundation (NRF) of Korea funded by the Ministry of Education (No. 2018R1A6A1A03025242 and No. 2018R1D1A1A09083353), a Research Grant of Kwangwoon University, Korea, in 2019, the Shandong Provincial Natural Science Foundation of China under Grant (ZR2017JL027), and the Zhejiang Lab (2019MC0AB03).

Notes

The authors declare no competing financial interest.

■ ABBREVIATIONS

IDC - interdigitated capacitor
APTES - 3-aminopropyltriethoxysilane
AFM - atomic force microscopy
ECL - electrochemiluminescence
ELISA - enzyme-linked immunosorbent assay
IFNγ - interferon γ
PCa - prostate cancer
PDMS - poly(dimethylsiloxane)
PSA - prostate-specific antigen
SEM - scanning electron microscopy
SPR - surface plasmon resonance
SERS - surface-enhanced Raman scattering
PBS - phosphate-buffered saline
POC - point of care
FT-IR - Fourier transform infrared spectroscopy
ADS - Advance Design System

■ REFERENCES

(1) Center, M. M.; Jemal, A.; Lortet-Tieulent, J.; Ward, E.; Ferlay, J.; Brawley, O.; Bray, F. International variation in prostate cancer incidence and mortality rates. *Eur. Urol.* **2012**, *61*, 1079−1092.

(2) Jung, K.-W.; Park, S.; Won, Y.-J.; Kong, H.-J.; Lee, J. Y.; Seo, H. G.; Lee, J.-S. Prediction of cancer incidence and mortality in Korea, 2012. *Cancer Res. Treat.* **2012**, *44*, 25.

(3) Kim, S. H.; Kim, S.; Joung, J. Y.; Kwon, W.-A.; Seo, H. K.; Chung, J.; Nam, B.-H.; Lee, K. H. Lifestyle risk prediction model for prostate cancer in a Korean population. *Cancer Res. Treat.* **2018**, *50*, 1194.

(4) Welch, H. G.; Gorski, D. H.; Albertsen, P. C. Trends in Metastatic Breast and Prostate Cancer. *New Engl. J. Med.* **2016**, *374*, 596.

(5) Ankerst, D. P.; Gelfond, J.; Goros, M.; Herrera, J.; Strobl, A.; Thompson, I. M., Jr; Hernandez, J.; Leach, R. J. Serial percent-free PSA in combination with PSA for population-based early detection of prostate cancer. *J. Urol.* **2016**, *196*, 355.

(6) Armbruster, D. A. Prostate-specific antigen: biochemistry, analytical methods, and clinical application. *Clin. Chem.* **1993**, *39*, 181−195.

(7) Zhou, A. M.; Tewari, P. C.; Bluestein, B. I.; Caldwell, G. W.; Larsen, F. L. Multiple forms of prostate-specific antigen in serum: differences in immunorecognition by monoclonal and polyclonal assays. *Clin. Chem.* **1993**, *39*, 2483−2491.

(8) Carter, H. B.; Albertsen, P. C.; Barry, M. J.; Etzioni, R.; Freedland, S. J.; Greene, K. L.; Holmberg, L.; Kantoff, P.; Konety, B. R.; Murad, M. H.; et al. Early detection of prostate cancer: AUA Guideline. *J. Urol.* **2013**, *190*, 419−426.

(9) Steuber, T.; O'Brien, M. F.; Lilja, H. Serum markers for prostate cancer: a rational approach to the literature. *Eur. Urol.* **2008**, *54*, 31−40.

(10) Liu, B.; Lu, L.; Hua, E.; Jiang, S.; Xie, G. Detection of the human prostate-specific antigen using an aptasensor with gold nanoparticles encapsulated by graphitized mesoporous carbon. *Microchim. Acta* **2012**, *178*, 163−170.

(11) Grönberg, H. Prostate cancer epidemiology. *Lancet* **2003**, *361*, 859−864.

(12) Roddam, A. W.; Duffy, M. J.; Hamdy, F. C.; Ward, A. M.; Patnick, J.; Price, C. P.; Rimmer, J.; Sturgeon, C.; White, P.; Allen, N. E. Use of prostate-specific antigen (PSA) isoforms for the detection of prostate cancer in men with a PSA level of 2−10 ng/ml: systematic review and meta-analysis. *Eur. Urol.* **2005**, *48*, 386−399.

(13) Healy, D. A.; Hayes, C. J.; Leonard, P.; McKenna, L.; O'Kennedy, R. Biosensor developments: application to prostate-specific antigen detection. *Trends Biotechnol.* **2007**, *25*, 125−131.

(14) D'Orazio, P. Biosensors in clinical chemistry—2011 update. *Clin. Chim. Acta* **2011**, *412*, 1749−1761.

(15) Bangar, M. A.; Shirale, D. J.; Chen, W.; Myung, N. V.; Mulchandani, A. Single conducting polymer nanowire chemiresistive label-free immunosensor for cancer biomarker. *Anal. Chem.* **2009**, *81*, 2168−2175.

(16) Graves, H.; Wehner, N.; Stamey, T. A. Ultrasensitive radioimmunoassay of prostate-specific antigen. *Clin. Chem.* **1992**, *38*, 735−742.

(17) Härmä, H.; Soukka, T.; Lönnberg, S.; Paukkunen, J.; Tarkkinen, P.; Lövgren, T. Zeptomole detection sensitivity of prostate-specific antigen in a rapid microtitre plate assay using time-resolved fluorescence. *Luminescence* **2000**, *15*, 351−355.

(18) Liang, J.; Yao, C.; Li, X.; Wu, Z.; Huang, C.; Fu, Q.; Lan, C.; Cao, D.; Tang, Y. Silver nanoprism etching-based plasmonic ELISA for the high sensitive detection of prostate-specific antigen. *Biosens. Bioelectron.* **2015**, *69*, 128−134.

(19) Breault-Turcot, J.; Poirier-Richard, H.-P.; Couture, M.; Pelechacz, D.; Masson, J.-F. Single chip SPR and fluorescent ELISA assay of prostate specific antigen. *Lab Chip* **2015**, *15*, 4433−4440.

(20) Liu, A.; Zhao, F.; Zhao, Y.; Shangguan, L.; Liu, S. A portable chemiluminescence imaging immunoassay for simultaneous detection of different isoforms of prostate specific antigen in serum. *Biosens. Bioelectron.* **2016**, *81*, 97−102.

(21) Gao, R.; Cheng, Z.; deMello, A. J.; Choo, J. Wash-free magnetic immunoassay of the PSA cancer marker using SERS and droplet microfluidics. *Lab Chip* **2016**, *16*, 1022−1029.

(22) Chuah, K.; Lai, L. M.; Goon, I. Y.; Parker, S. G.; Amal, R.; Gooding, J. J. Ultrasensitive electrochemical detection of prostate-specific antigen (PSA) using gold-coated magnetic nanoparticles as 'dispersible electrodes'. *Chem. Commun.* **2012**, *48*, 3503−3505.

(23) Lee, J. H.; Rho, J.-E. R.; Rho, T.-H. D.; Newby, J. G. Advent of innovative chemiluminescent enzyme immunoassay. *Biosens. Bioelectron.* **2010**, *26*, 377−382.
(24) Panini, N. V.; Messina, G. A.; Salinas, E.; Fernández, H.; Raba, J. Integrated microfluidic systems with an immunosensor modified with carbon nanotubes for detection of prostate specific antigen (PSA) in human serum samples. *Biosens. Bioelectron.* **2008**, *23*, 1145−1151.
(25) Kumar, P.; Kim, K.-H.; Deep, A. Recent advancements in sensing techniques based on functional materials for organophosphate pesticides. *Biosens. Bioelectron.* **2015**, *70*, 469−481.
(26) Kong, R.-M.; Ding, L.; Wang, Z.; You, J.; Qu, F. A novel aptamer-functionalized MoS 2 nanosheet fluorescent biosensor for sensitive detection of prostate specific antigen. *Anal. Bioanal.Chem.* **2015**, *407*, 369−377.
(27) Choi, H. K.; Lee, J. H. Role of magnetic Fe 3 O 4 graphene oxide in chemiluminescent aptasensors capable of sensing tumor markers in human serum. *Anal. Methods* **2013**, *5*, 6964−6968.
(28) Souada, M.; Piro, B.; Reisberg, S.; Anquetin, G.; Noël, V.; Pham, M. Label-free electrochemical detection of prostate-specific antigen based on nucleic acid aptamer. *Biosens. Bioelectron.* **2015**, *68*, 49−54.
(29) Jolly, P.; Tamboli, V.; Harniman, R. L.; Estrela, P.; Allender, C. J.; Bowen, J. L. Aptamer−MIP hybrid receptor for highly sensitive electrochemical detection of prostate specific antigen. *Biosens. Bioelectron.* **2016**, *75*, 188−195.
(30) Chandola, C.; Kalme, S.; Casteleijn, M. G.; Urtti, A.; Neerathilingam, M. Application of aptamers in diagnostics, drug-delivery and imaging. *J. Biosci.* **2016**, *41*, 535−561.
(31) Song, S.; Wang, L.; Li, J.; Fan, C.; Zhao, J. Aptamer-based biosensors. *TrAC, Trends Anal. Chem.* **2008**, *27*, 108−117.
(32) Zheng, X.; Li, L.; Cui, K.; Zhang, Y.; Zhang, L.; Ge, S.; Yu, J. Ultrasensitive enzyme-free biosensor by coupling cyclodextrin functionalized Au nanoparticles and high-performance Au-paper electrode. *ACS Appl. Mater. Interfaces* **2018**, *10*, 3333−3340.
(33) Yang, L.; Li, N.; Wang, K.; Hai, X.; Liu, J.; Dang, F. A novel peptide/Fe3O4@ SiO2-Au nanocomposite-based fluorescence biosensor for the highly selective and sensitive detection of prostate-specific antigen. *Talanta* **2018**, *179*, 531−537.
(34) Xu, T.; Song, Y.; Gao, W.; Wu, T.; Xu, L.-P.; Zhang, X.; Wang, S. Superwettable electrochemical biosensor toward detection of cancer biomarkers. *ACS Sens.* **2018**, *3*, 72−78.
(35) Spain, E.; Gilgunn, S.; Sharma, S.; Adamson, K.; Carthy, E.; O'Kennedy, R.; Forster, R. J. Detection of prostate specific antigen based on electrocatalytic platinum nanoparticles conjugated to a recombinant scFv antibody. *Biosens. Bioelectron.* **2016**, *77*, 759−766.
(36) Kong, T.; Flanigan, S.; Weinstein, M.; Kalwa, U.; Legner, C.; Pandey, S. A fast, reconfigurable flow switch for paper microfluidics based on selective wetting of folded paper actuator strips. *Lab Chip* **2017**, *17*, 3621−3633.
(37) Messina, M.; Meli, C.; Conoci, S.; Petralia, S. A facile method for urinary phenylalanine measurement on paper-based lab-on-chip for PKU therapy monitoring. *Analyst* **2017**, *142*, 4629−4632.
(38) Li, W.; Shi, Z.; Fang, C.; Lu, Y.; Yu, L.; Li, C. M. Integration of paper and micropipette tip to build a "sample-in, answer-out" point-of-care device. *Microfluid. Nanofluid.* **2017**, *21*, No. 71.
(39) Salim, B.; Athira, M.; Kandaswamy, A.; Vijayakumar, M.; Saravanan, T.; Sairam, T. Microfluidic device for novel breast cancer screening by blood test using miRNA beacon probe. *Biomed. Microdevices* **2017**, *19*, No. 89.
(40) Tsai, M.-Z.; Hsiung, C.-T.; Chen, Y.; Huang, C.-S.; Hsu, H.-Y.; Hsieh, P.-Y. Real-time CRP detection from whole blood using micropost-embedded microfluidic chip incorporated with label-free biosensor. *Analyst* **2018**, *143*, 503−510.
(41) Matta, D. P.; Tripathy, S.; Vanjari, S. R. K.; Sharma, C. S.; Singh, S. G. An ultrasensitive label free nanobiosensor platform for the detection of cardiac biomarkers. *Biomed. Microdevices* **2016**, *18*, No. 111.
(42) Castiello, F. R.; Tabrizian, M. Multiplex Surface Plasmon Resonance Imaging-Based Biosensor for Human Pancreatic Islets Hormones Quantification. *Anal. Chem.* **2018**, *90*, 3132−3139.
(43) Chuang, C.-H.; Du, Y.-C.; Wu, T.-F.; Chen, C.-H.; Lee, D.-H.; Chen, S.-M.; Huang, T.-C.; Wu, H.-P.; Shaikh, M. O. Immunosensor for the ultrasensitive and quantitative detection of bladder cancer in point of care testing. *Biosens. Bioelectron.* **2016**, *84*, 126−132.
(44) Ding, S.; Mosher, C.; Lee, X. Y.; Das, S. R.; Cargill, A. A.; Tang, X.; Chen, B.; McLamore, E. S.; Gomes, C.; Hostetter, J. M.; Claussen, J. C. Rapid and label-free detection of interferon gamma via an electrochemical aptasensor comprising a ternary surface monolayer on a gold interdigitated electrode array. *ACS Sens.* **2017**, *2*, 210−217.
(45) Cui, W.; He, M.; Mu, L.; Lin, Z.; Wang, Y.; Pang, W.; Reed, M.; Duan, X. Cellphone-enabled microwell-based microbead aggregation assay for portable biomarker detection. *ACS Sens.* **2018**, *3*, 432−440.
(46) Ji, S.; Lee, M.; Kim, D. Detection of early stage prostate cancer by using a simple carbon nanotube@ paper biosensor. *Biosens. Bioelectron.* **2018**, *102*, 345−350.
(47) Shirzadfar, H.; Khanahmadi, M. Application of Biomarkers and Biosensors to Detect and Track Pathogenic Agents. *Int. J. Anal. Techn.* **2018**, 1−5.
(48) Sypabekova, M.; Korganbayev, S.; González-Vila, Á.; Caucheteur, C.; Shaimerdenova, M.; Ayupova, T.; Bekmurzayeva, A.; Vangelista, L.; Tosi, D. Functionalized etched tilted fiber Bragg grating aptasensor for label-free protein detection. *Biosens. Bioelectron.* **2019**, *146*, No. 111765.
(49) Yoo, Y. K.; Kim, J.; Kim, G.; Kim, Y. S.; Kim, H. Y.; Lee, S.; Cho, W. W.; Kim, S.; Lee, S.-M.; Lee, B. C.; et al. A highly sensitive plasma-based amyloid-β detection system through medium-changing and noise cancellation system for early diagnosis of the Alzheimer's disease. *Sci. Rep.* **2017**, *7*, No. 8882.
(50) Kim, N.; Dhakal, R.; Adhikari, K.; Kim, E.; Wang, C. A reusable robust radio frequency biosensor using microwave resonator by integrated passive device technology for quantitative detection of glucose level. *Biosens. Bioelectron.* **2015**, *67*, 687−693.
(51) Liang, J.-G.; Wang, C.; Yao, Z.; Liu, M.-Q.; Kim, H.-K.; Oh, J.-M.; Kim, N.-Y. Preparation of ultrasensitive humidity-sensing films by aerosol deposition. *ACS Appl. Mater. Interfaces* **2018**, *10*, 851−863.
(52) Kim, E.-S.; Liang, J.-G.; Wang, C.; Cho, M.-Y.; Oh, J.-M.; Kim, N.-Y. Inter-digital capacitors with aerosol-deposited high-K dielectric layer for highest capacitance value in capacitive super-sensing applications. *Sci. Rep.* **2019**, *9*, No. 680.
(53) Vashist, S. K.; Lam, E.; Hrapovic, S.; Male, K. B.; Luong, J. H. Immobilization of antibodies and enzymes on 3-aminopropyltriethoxysilane-functionalized bioanalytical platforms for biosensors and diagnostics. *Chem. Rev.* **2014**, *114*, 11083−11130.

https://dx.doi.org/10.1021/acsabm.0c01002
ACS Appl. Bio Mater. XXXX, XXX, XXX−XXX